OPTIMUM ISOLATION DESIGN FOR HIGHWAY BRIDGES USING FRAGILITY FUNCTION METHOD

J. Zhang[1], Y. Huo[2]

[1] *Assistant Professor,* [2] *Graduate Student Researcher, Department of Civil and Environmental Engineering ,*
University of California, Los Angeles, USA
Email: zhangj@ucla.edu; huoyili@ucla.edu

ABSTRACT :

Seismic isolation can be used to improve the seismic response and reduce damages of bridges. This paper aims to use the performance-based evaluation approach to investigate the performance of highway bridges with base isolation. Fragility functions are derived for typical base-isolated highway bridges using a simplified two dimensional numerical model representing the transverse response of bridges. The nonlinear models for piers and isolation devices are incorporated and various combinations of isolation parameters, e.g. elastic stiffness, characteristic strength and post-yielding stiffness representing common types of isolation devices are evaluated. Fragility curves are derived based on nonlinear time history analyses using a suite of 250 recorded earthquake motions in California. Damage criteria for both pier and isolation device are established to relate the response quantities to damage index of the bridge. The derived fragility functions define the probability of exceeding a predefined performance state at varying levels of earthquake intensity. By evaluating the earthquake intensity required to achieve specified damage states of base-isolated bridges, the optimum parameters of isolation devices are identified as function of structural properties. The study shows that the mechanical properties of isolation devices play an important role to the bridge response. The fragility function method provides an effective way to achieve the optimum design to minimize the damaging potential of bridges while incorporating the uncertainties in ground motions and variability of structural properties.

KEYWORDS: bridge, isolation, fragility function, optimal parameter, efficiency

1. INTRODUCTION

Highway bridges are the most common type of bridges and crucial components of transportation networks. They are susceptible to damages under major earthquakes, which subsequently cause significant direct or indirect economic impact. In recent years, seismic isolation devices have been used to improve the seismic response and reduce damage of bridges for both new and retrofitting applications (Buckle and Mayes 1990; Naiem and Kelly 1999; Imbsen 2001). With its flexibility and energy dissipation mechanism, isolation devices can lengthen the natural period of bridge to avoid the dominant frequency of earthquake input and provide extra damping ratio into the bridge system. However, isolation devices possess various mechanical properties and their behavior is often highly nonlinear and sometimes frequency and rate dependent. Furthermore, it has been found that the response of seismic-isolated bridges is a function of ground motion and properties of isolator (Dicleli and Buddaram 2006). Therefore, the successful implementation of base isolation technique requires careful selection of isolation devices based on the structural/geotechnical parameters, ground motion characteristics and performance objectives. As remarked by Priestly et al (1996), the possible wide selection of design parameters makes that the design of isolated bridge is still more art than a combination of rules.

Several studies have evaluated the effectiveness and optimal design of isolation devices on bridges through deterministic methods (Ghobarah and Ali 1988; Jangid 2005, 2007; Kunde and Jangid 2006). The effects of both structural and isolator properties on bridge responses were identified in these studies. By examining bridge responses under six near-fault earthquake motions, Jangid (2005, 2007) identified that the optimum friction coefficient should be 0.05-0.15 for friction pendulum system while the optimum characteristic strength of lead-rubber bearing should be 10-15% of the total weight of the structure. Since the effectiveness of seismic isolation highly depends on the frequency characteristics of structures and earthquake motions, the deterministic approach, employing seismic spectra or a few ground motion records as inputs, has difficulty to account for the uncertainties of earthquake motions and to obtain a comprehensive evaluation. Recent theoretical development of fragility function method makes it possible to probabilistically deal with the uncertainties and to evaluate global bridge damage under earthquake. Under the fragility function framework, several recent studies have looked into the effects of retrofitting measures and seismic isolation on seismic response of bridges. Karim and Yamazaki (2007) developed a simplified approach to derive fragility functions of isolated bridges and demonstrated the contribution of isolators on reducing damage probability of bridge columns. The study by Padgett and DesRoches (2008) compared the fragility functions of retrofitted bridges using various retrofit measures and found that the bridge system fragility should be used to correctly evaluate the retrofit impact on the damage states. Recent study by Zhang and Huo (2008) illustrated the isolation effects with global level fragility functions of bridges.

This paper employs the fragility function method as a tool to investigate the efficiency of isolation devices and to evaluate the influence of the mechanic properties of isolation devices on mitigating damage potential of bridges. A global damage index is devised based on component damage indexes of bridge piers and isolation bearings. The fragility functions of bridges with various isolation devices are derived and compared. The effects of isolator properties on bridge damage potential are identified and parameters for optimal isolation design are provided.

2. FRAGILITY FUNCTIONS OF BRIDGES

2.1. Numerical Models for Bridge and Isolation Device

The prototype bridge used in this study is adapted from the Mendocino Overcrossing in California, which is a typical highway bridge built before 1971 (see Figure 1a). It is a four-span continuous concrete box-girder bridge with monolithic abutments and supported by single column piers. The fundamental mode is in transver direction with a period of $T_1=0.35s$. Since the bridge is not skewed, i.e. resulting in minimal 3D effects, a simplified 2D model (shown in Figure 1b) is built to represent the transverse response of the bridge. The comparison between the seismic responses of the original 3D bridge model and that of the 2D model shows that the 2D model is adequate and efficient. Numerical models are generated in software platform OpenSees (Mazzoni et al. 2006). Nonlinear fiber section beam elements are used to model the pier columns.

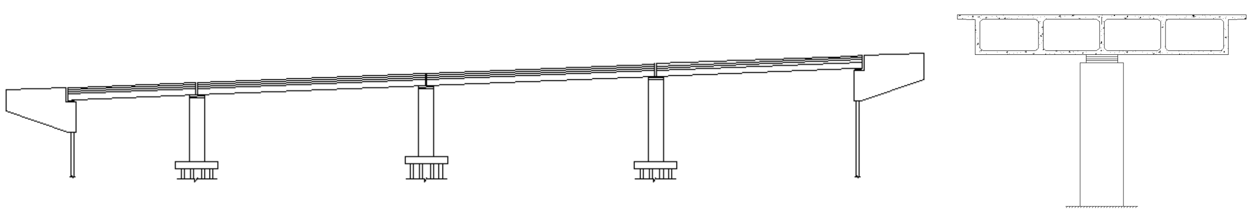

(a) Elevation view of the Mendocino Overcrossing, CA (b) 2D model

Figure 1 Sketch of the Mendocino Overcrossing and 2D model of the bridge

Three most common types of isolation devices, i.e. elastomeric rubber bearing (ERB), lead-rubber bearing (LRB) and friction pendulum bearing (FPS), are investigated in this paper. Figure 2a-c shows the sketches and the corresponding cyclic behaviors of these isolators. Although their behaviors are different from each other, one can use a bilinear model as shown in Figure 2d to represent their behavior (Naeim and Kelly, 1999; Kumar and Paul, 2007). This bilinear model can be completely described by elastic stiffness K_1, characteristic strength Q and post-yielding stiffness K_2. The parameters and formulas for bilinear modeling of typical isolation devices are summarized in Table 2.1. As shown in the table, the characteristic strength Q and post-yielding stiffness K_2 can be determined with physical property parameters, while the elastic stiffness K_1 are usually evaluated through empirical estimation of the stiffness ratio N, which is the ratio between elastic stiffness and post-yielding stiffness ($N=K_1/K_2$).

In order to normalize the mechanical properties of isolation devices with that of structural properties, the force-displacement relation of the pier column in the bridge model is also regressed with bilinear curve and the corresponding elastic stiffness, characteristic strength and post-yielding stiffness are extracted. In describing the parameters, subscript “C” is used to indicate column properties while subscript “B” to indicate bearing properties.

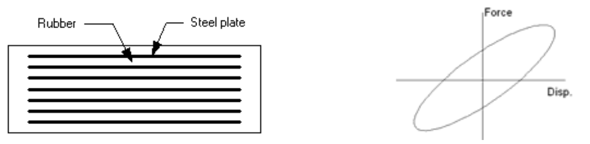

(a) Sketch and cyclic loop of elastomeric rubber bearing (ERB)

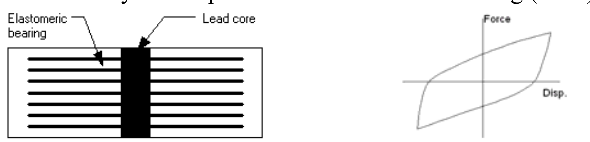

(b) Sketch and cyclic loop of lead-plug rubber bearing (LRB)

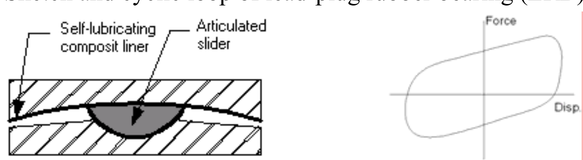

(c) Sketch and cyclic loop of friction pendulum bearing (FPS)

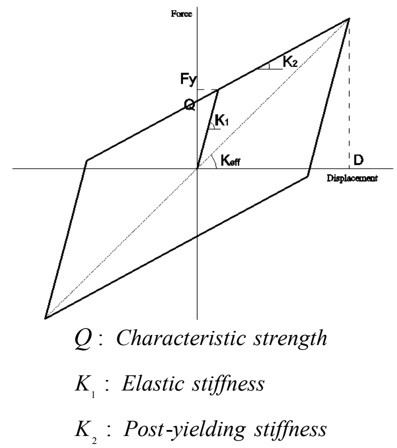

(d) Bilinear model

Figure 2 Sketch, cyclic behavior and bilinear modeling of typical isolation devices

Table 2.1 Bilinear modeling parameters for typical isolation devices

Isolation Type	Elastic stiffness K_1	Characteristic strength Q	Post-yielding stiffness K_2
ERB	$K_1=NK_2$ (N=5 - 15)	From hysteresis loop	$K_2=GA/\sum t_r$
LRB	$K_1=NK_2$ (N=15 - 30)	$F_y=f_yA_{Lead}$	$K_2=(1.15\sim1.20)GA/\sum t_r$
FPS	$K_1=NK_2$ (N=50 - 100)	$Q=\mu W$	$K_2=W/R$

2.2. Fragility Function Methodology

The fragility functions of bridges can be numerically derived using a large number of nonlinear time history analyses that account for the uncertainties in both seismic input motions and structural properties. Two computational methods, namely the probabilistic seismic demand analysis (PSDA) and the incremental dynamic analysis (IDA) are widely used to derive the fragility functions. PSDA relates the engineering demand parameter (EDP) to the intensity measure (IM) of earthquake inputs through an logarithm relationship and obtains the fragility function parameters by assuming the form of fragility distribution (Mackie and Stojadinović, 2003, 2007). IDA derives the fragility functions by counting the damage cases for each IM level from the time history analyses of bridges using ground motions scaled to the same intensity level (Karim and Yamazaki, 2001).

In this paper, 250 sets of earthquake records are selected for both PSDA and IDA and the records are input in transverse, longitudinal and vertical direction simultaneously during analyses. Peak ground acceleration (PGA) is adopted as IM for earthquake input. The damage in pier columns and bearings are monitored and Table 2.2 lists the EDP, damage index (DI), damage state (DS) and corresponding limit state (LS) definitions for these two critical components. During earthquake, piers and bearings can experience different damage states, leading to a comprehensive damage state which is hard to be described by only one component DI. Previous studies suggest that a system fragility can be derived based on the functionality or repair cost after earthquake (Mackie and Stojadinović, 2007), or be generated based on component level fragility (Nielson and DesRoches, 2007). In this study, a composite damage state (DS) is developed as shown in Eqn. 2.1. The proportion ratio 0.75 for columns and 0.25 for isolation devices are determined synthetically by considering the relative component importance for load-carrying capacity during earthquake and the repair cost after earthquake.

$$DS = \begin{cases} \text{int}\left(0.75 \cdot DS_{Pier} + 0.25 \cdot DS_{Bearing}\right) & DS_{Pier}, DS_{Bearing} < 4 \\ 4 & DS_{Pier} \text{ or } DS_{Pier} = 4 \end{cases} \tag{2.1}$$

Table 2.2 Probability of parameters of soil profile and foundation modeling

	EDP or DI definition	Slight damage (DS=1)	Moderate damage (DS=2)	Extensive damage (DS=3)	Collapse damage (DS=4)
Pier column (Choi et al, 2004)	Section ductility μ	μ>1	μ>2	μ>4	μ>7
Bearing	Shear strain γ	γ>100%	γ>150%	γ>200%	γ>400%

2.3. Fragility Functions of Non-Isolated Bridges

For non-isolated bridge model, PSDA method plots the EDP (section ductility) and IM (peak ground acceleration) pairs of 250 simulation cases in Figure 3a and a linear regression with logarithm values are achieved to relate EDP and IM. With this relationship and assumptions that the fragility curves follow a cumulative normal or lognormal distribution function, fragility curves are generated as shown in Figure 3b. IDA is conducted also with 250 sets of records at 25 PGA levels ranging from 0.06g to 1.5g (6250 simulation cases). The cumulative normal distribution function is assumed for regression analysis of the simulation data. The generated fragility curves based on regression are plotted and compared with PSDA curves in Figure 3b. It is shown that the PSDA and IDA methods yield comparable fragility curves. However, IDA method is considered to be more reliable and is adopted in this study. During the regression process, one obtains the mean and standard deviation of earthquake intensity required to achieve certain damage state. The mean value μ_{IM} of the regression cumulative normal distribution functions is a good indicator of the bridge damage potential as it controls the location of fragility curves directly. With similar standard deviation σ value, fragility curves with bigger mean value μ_{IM} represent smaller damage probability, i.e. better performance under seismic loading.

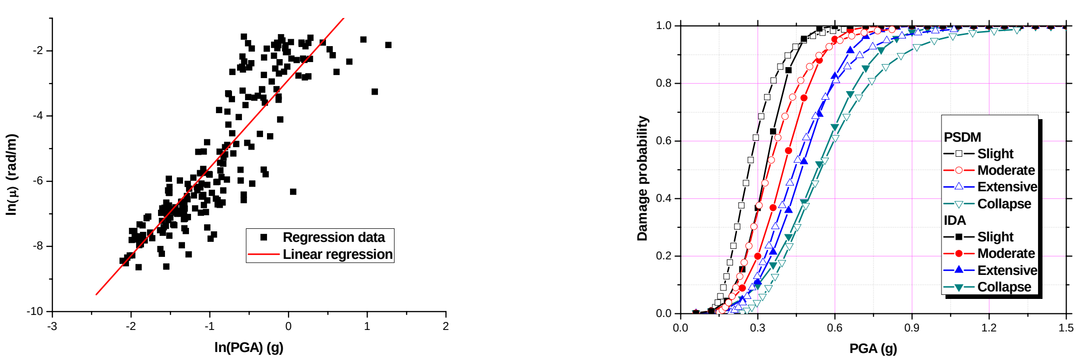

(a) PSDA results (b) PSDA and IDA Fragility curves

Figure 3 Fragility analyses of non-isolated bridge with PSDA or IDA

2.4. Fragility Functions of Isolated Bridges

The prototype bridge is retrofitted with isolation devices, which are designed following a general design process (Naeim and Kelly, 1999) and their parameters are selected as $K_{1,B}/K_{1,C}$=0.65, Q_B/Q_C=0.85 and $K_{2,B}/K_{1,B}$=1/50. The component level and bridge level fragility curves are derived with IDA and compared with that of non-isolated model in Figure 4. The isolated bridge has much smaller damage probability for all four damage states. The pier columns in the isolated model experience much less damage than that in the un-isolated model. However, the bearings in isolated bridges experience larger displacement or damage than that of columns. This observation indicates that the global damage state can be underestimated if only the damages in columns are considered. The fragility curves using composite DI are the proportional summation of the two component level fragility curves. They locate between the component fragility curves and appropriately capture the global damage states of the entire bridge system.

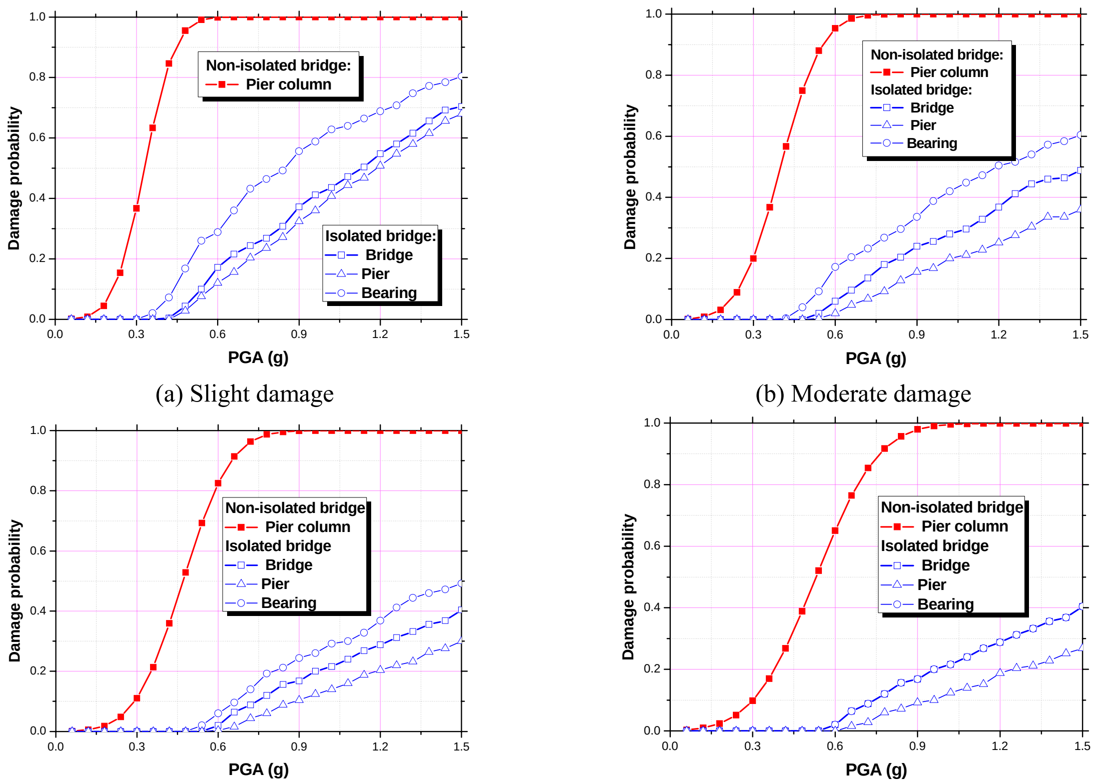

(a) Slight damage

(b) Moderate damage

(c) Extensive damage

(d) Collapse damage

Figure 4 Fragility curves of isolated bridge with component and composite DIs

3. OPTIMUM ISOLATION DESIGN

In order to investigate the influence of mechanical properties of isolation devices on the dynamic response and damage probability of bridges as well as identifying the optimum isolation design, an extensive parametric study has been conducted in this section using the same prototype bridge. Since different isolation devices posses different stiffness ratio $N=K_{1,B}/K_{2,B}$, it is chosen to be 10, 30, 50 and 70 respectively to reflect the different isolation type in this study. With the specified N values, the bearing elastic stiffness $K_{1,B}$ is varied from 0.15 to 1.65 times of the column elastic stiffness $K_{1,C}$, and the bearing yielding strength Q_B is varied from 0.15 to 0.95 times of the column yielding strength Q_C. The fragility functions for each model with various combinations of isolation parameters are derived for each damage state and the mean values of earthquake intensity required for reaching the damage states are recorded and compared to show the efficiency of isolation. As mentioned before, the higher the mean value, the smaller damage probability. This implies the better isolation design.

Figure 5 plots the mean value of earthquake intensity as function of Q_B/Q_C and $K_{1,B}/K_{1,C}$ to reach the different damage states for the case when stiffness ratio N is kept as 30 which can be commonly observed in ERB and LRB. The peak points on the contours represent the biggest mean values of earthquake intensity required, which also correspond to the best structural performance. The bearing parameters at these peak points represent the optimal design. Although the locations of the peak points are slightly different in four damage states (Figure 5a-d), it can be seen that bearing with $Q_B=0.55Q_C$ and $K_{1,B}=0.75K_{1,C}$ would be a good choice for retrofitting the prototype bridge.

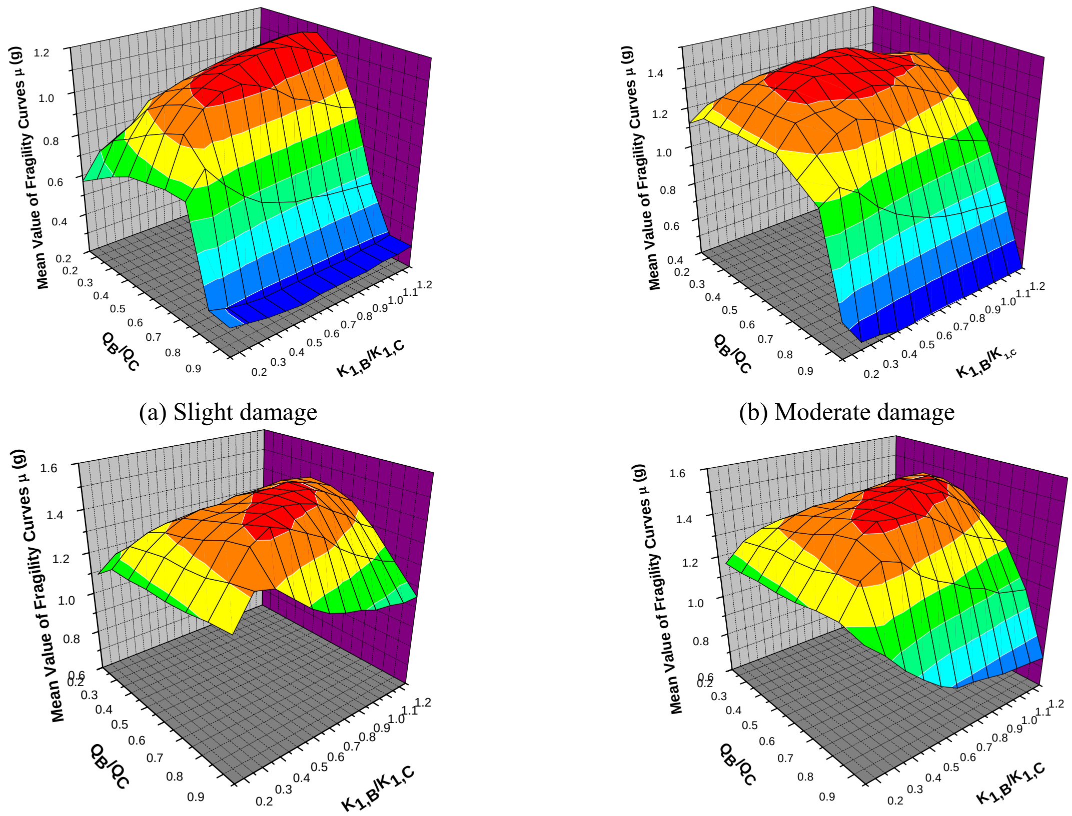

(a) Slight damage (b) Moderate damage

(c) Extensive damage (d) Collapse damage

Figure 5 Influence of Q_B and $K_{1,B}$ of isolation devices (N=30) on mean values of bridge fragility curves

Similarly, the optimum isolation design can be identified for isolation devices with stiffness ratios of N=10, 50 and 70 respectively. The results are summarized in Table 3.1. The data suggest that the optimal bearing characteristic strength Q_B is around $0.55Q_C$ and it is not sensitive with stiffness ratio N. Since it is very likely that the $K_{1,B}/K_{1,C}$ increases proportionally with stiffness ratio N, the results imply that the elastic stiffness $K_{1,B}$ may not be very important while $K_{2,B}$ probably plays a much more crucial role for optimal design of isolation devices.

To validate the above presumption, further parameter studies are carried out. The analysis keeps Q_B as $0.55Q_C$ and varies $K_{1,B}$ and $K_{2,B}$ separately to study their effects on bridge performance. Figure 6 plots the mean value of earthquake intensity as function of $K_{1,B}/K_{1,C}$ and $K_{2,B}/K_{2,C}$ to reach the different damage states. It is seen that the the bridge damage probability is not sensitive to $K_{1,B}$. Consequently, the $K_{1,B}$ can be maintained as around $1.0K_{1,C}$ while the other two parameters ($K_{2,B}$ and Q) need to be chosen carefully.

Table 3.1 Optimal design parameters of isolation devices with different stiffness ratio N

Stiffness ratio $N=K_{2,B}/K_{1,B}$		10	30	50	70
Slight	Q_B/Q_C	0.45	0.55	0.55	0.55
	$K_{1,B}/K_{1,C}$	0.35	0.85	1.25	1.55
Moderate	Q_B/Q_C	0.45	0.45	0.45	0.45
	$K_{1,B}/K_{1,C}$	0.25	0.65	1.05	1.35
Extensive	Q_B/Q_C	0.45	0.45	0.65	0.65
	$K_{1,B}/K_{1,C}$	0.35	0.85	1.15	1.55
Collapse	Q_B/Q_C	0.45	0.65	0.65	0.65
	$K_{1,B}/K_{1,C}$	0.35	0.75	1.15	1.65

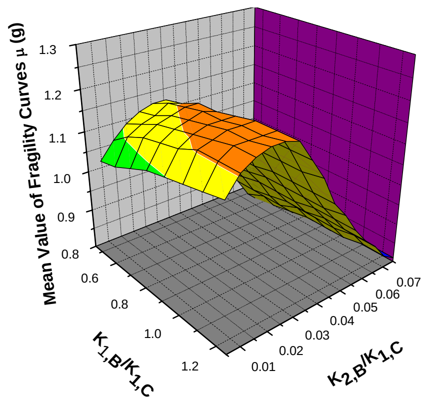

(a) Slight damage

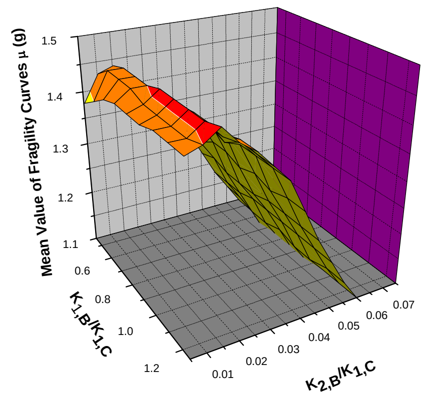

(b) Moderate damage

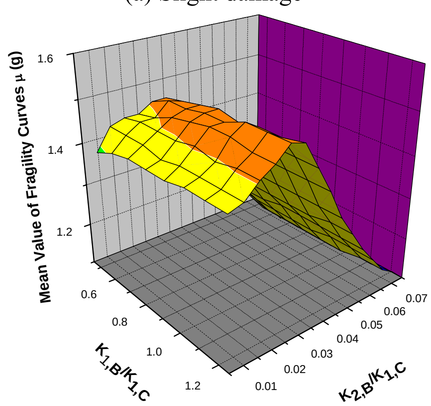

(c) Extensive damage

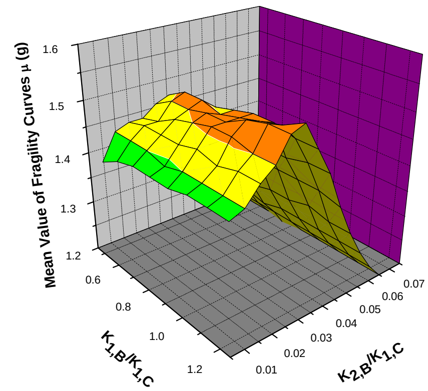

(d) Collapse damage

Figure 6 Influence of K_1 and K_2 on mean values of bridge fragility curves

For bridges with different fundamental periods, the optimum isolation design parameters are also identified using the fragility function method. The results are summarized in Table 3.2. These identified optimum isolation design parameters provide an efficient guidance in selecting the isolation devices based on structural properties of the bridge.

Table 3.2 Optimal design parameters of isolation devices for bridges with various fundamental periods

Structural periods T (s)		0.35	0.45	0.55	0.65	0.75
Slight	Q_B/Q_C	0.55	0.55	0.65	0.75	0.85
	$K_{2,B}/K_{1,C}$	0.028	0.035	0.038	0.038	0.042
Moderate	Q_B/Q_C	0.55	0.55	0.65	0.65	0.75
	$K_{2,B}/K_{1,C}$	0.028	0.025	0.038	0.025	0.028
Extensive	Q_B/Q_C	0.55	0.75	0.55	0.85	0.85
	$K_{2,B}/K_{1,C}$	0.035	0.025	0.032	0.032	0.035
Collapse	Q_B/Q_C	0.55	0.75	0.55	0.85	0.85
	$K_{2,B}/K_{1,C}$	0.038	0.025	0.028	0.035	0.035

4. CONCLUSION

This paper utilizes fragility function method to investigate the optimum isolation design for highway bridges. The fragility curves are generated for un-isolated and isolated bridges using a large number of nonlinear time history analyses. A composite damage index is developed to measure the global damage states of bridge systems. The study shows that isolation devices can drastically reduce the damage probability of bridges. In order to identify the optimum isolation design parameters, an extensive parametric study was carried out under the fragility analysis framework to evaluate the damage potential of isolated bridges with various isolation devices that possess different combinations of elastic stiffness, post-yielding stiffness and characteristic strength. The results show that the bridge will experience the minimal damage when the characteristic strength Q_B of isolation devices is about $0.55\sim0.85Q_C$ and the post-yielding stiffness $K_{2,B}$ is about $0.025\text{-}0.040K_{1,C}$. The elastic stiffness of bearing $K_{1,B}$ is found to be less sensitive as long as it is close to the elastic stiffness of column. The study offers an efficient way to select optimum isolation design parameters based on structural properties of bridges, e.g. fundamental period or elastic column stiffness.

ACKNOWLEDGEMENT

Partial funding for this work is provided by the Pacific Earthquake Engineering Research Center Lifelines program under project task No. 9C. The study utilized the computational resource at the San Diego Supercomputer Center (SDSC) through cyber-infrastructure resource allocation program.

REFERENCES

Buckle, I.G. and Mayes, R.L. (1990) Seismic isolation: history, application and performance – a world view. *Earthquake Spectra* **6:2**, 161-201.

Choi, E., DesRoches, R. and Nielson, B. (2004). Seismic fragility of typical bridges in moderate seismic zones. *Engineering Structures* **26**, 187-199.

Dicleli, M. and Baddaram, S. (2006). Effect of isolator and ground motion characteristics on the performance of seismic-isolated bridges. *Earthquake Engineering and Structural Dynamics*, **35**, 233-250.

Ghobarah, A. and Ali, H.M. (1988). Seismic performance of highway bridges. *Engineering Structures* **10**, 157-166.

Imbsen, R.A. (2001). Use of isolation for seismic retrofitting bridges. *Journal of Bridge Engineering* **6:6**, 425-438.

Jangid, R.S. (2005). Optimal friction pendulum system for near-fault motions. *Engineering Structures* **27**, 349-359.

Jangid, R.S. (2007). Optimal lead-rubber isolation bearings for near-fault motions. *Engineering Structures* **29**, 2503-2513.

Karim, K.R. and Yamazaki, F. (2001). Effect of earthquake ground motions on fragility curves of highway bridge piers based on numerical simulation. *Earthquake Engineering and Structural Dynamics* **30**, 1839-1856.

Karim, K.R. and Yamazaki, F. (2007). Effect of isolation on fragility curves of highway bridges based on simplified approach. *Soil Dynamics and Earthquake Engineering* **27:4,** 14-426.

Kumar, P.T.V. and Paul, D.K. (2007). Force-deformation behavior of isolation bearings. *Journal of Bridge Engineering* **12:4**, 527-529.

Kunde, M.C. and Jangid, R.S. (2006). Effects of pier and deck flexibility on the seismic response of the isolated bridges. *Journal of Bridge Engineering* **11**, 109-121.

Mackie, K. and Stojadinović, B. (2003). Seismic demands for performance-based design of bridges. *PEER Report No. 2003/16.* Pacific Earthquake Engineering Research Center, University of California, Berkeley, USA.

Mackie, K. and Stojadinović, B. (2007). Performance-based seismic bridge design for damage and loss limit states. *Earthquake Engineering and Structural Dynamics* **36:13**, 1953-1971.

Naeim, F. and Kelly, J.M. (1999). Design of Seismic Isolated Structures: From Theory to Practice, John Wiley & Sons, New York, USA.

Nielson, B.G. and DesRoches, R. (2007). Seismic fragility methodology for highway bridges using a component level approach. *Earthquake Engineering and Structural Dynamics* **36**, 823-839.

Mazzoni, S., McKenna, F., Scott, M.H., and Fenves, G.L. (2006). OpenSees Command Language Manual. University of California, Berkeley, USA.

Padgett, J.E. and DesRoches, R. (2008). Methodology for the development of analytical fragility curves for retrofitted bridges. *Earthquake Engineering and Structural Dynamics* **37:8**, 1157-1174.

Priestley, M.J.N., Seible, F. and Calvi, G.M. (1996). Seismic Design and Retrofit of Bridges, John Wiley & Sons, New York, USA.

Zhang, J. and Huo, Y. (2008). Fragility function of base isolated highway bridges. *Structure Congress'08*, Vancouver, Canada, April, 2008.